ELSEVIER

Journal of Nuclear Materials 279 (2000) 118–126

journal of nuclear materials

www.elsevier.nl/locate/jnucmat

XPS and XRD studies of (Th,U)O_2 fuel corrosion in water

S. Sunder [a,*], N.H. Miller [b]

[a] *Atomic Energy of Canada Limited, Chalk River Laboratories, Fuel Safety Branch, Chalk River, ON, Canada, K0J 1J0*
[b] *Atomic Energy of Canada Limited, Whiteshell Laboratories, Pinawa, MB, Canada, R0E 1L0*

Received 21 May 1999; accepted 17 July 1999

Abstract

Dissolution and corrosion of (Th,U)O_2 fuel was investigated at room temperature and near 100°C in near neutral and acidic water (pH 3) to evaluate the suitability of irradiated UO_2-doped thoria as a waste form for direct geological disposal. X-ray photoelectron spectroscopy and X-ray diffraction were used to study oxidation of (Th,U)O_2 fuel. The uranium in the surface of (Th,U)O_2 fuel undergoes oxidation similar to that observed in UO_2 fuel under similar conditions. Nevertheless, the dissolution rate of uranium from (Th,U)O_2 fuel in aerated solutions is much lower than that from UO_2 fuel under similar conditions. These studies suggest that a properly prepared (Th,U)O_2 fuel can be an acceptable waste-form for permanent geological disposal. Crown copyright © 2000 Published by Elsevier Science B.V. All rights reserved.

1. Introduction

Thoria based nuclear fuels are being considered for use in CANDU reactors [1]. The CANDU reactor has the capability to use thoria based fuels because its excellent neutron economy, channel design and on-power refueling allow a high degree of fuel-cycle flexibility. One reason for the interest in thoria as a nuclear fuel is the potential of burning weapons' plutonium in a thoria-based matrix [2,3]. Also, the high relative abundance of thorium minerals compared to uranium minerals makes the thorium fuel cycle attractive to countries with significant thorium reserves.

Natural thorium does not have a fissile isotope. Therefore, thoria is generally mixed with another actinide oxide, containing a fissile isotope (e.g., $^{235}UO_2$ or $^{239}PuO_2$), for its use as a fuel in a nuclear reactor. The majority of the fissile isotopes (^{235}U or ^{239}Pu) present in the thoria fuel are then "burned-out" during its stay in the reactor, making this an attractive option for dispositioning weapons' plutonium. The fissile component of the used thoria fuel mainly consists of ^{233}U formed by the transformation of ^{233}Th. ^{233}Th is formed by an absorption of a neutron by ^{232}Th, the main isotope of thorium.

If thoria fuel is to be used as a nuclear fuel, one needs to know the behavior of (Th,U)O_2 in contact with water-both for storage (in a water pool) or disposal (in a geologic vault). Thoria (ThO_2) is very insoluble in water and does not undergo oxidation beyond its +4 oxidation state [4–6]. However, UO_2 does undergo oxidation beyond its +4 oxidation state, and uranium oxides with U in the higher (+6) oxidation state have higher solubility than UO_2 [7,8]. Although there are several studies on the dissolution of (Th,U)O_2 fuel in strongly acidic solutions [9], very few experimental results are available on the behavior of (Th,U)O_2 fuel in near neutral conditions expected during the storage or disposal of the used fuel. Here, we describe the results of our experiments on the dissolution of (Th,U)O_2 fuel in pure water and in slightly acidic water (pH 3). Changes in the surface oxidation of (Th,U)O_2 samples used in these tests were investigated using X-ray photoelectron spectroscopy (XPS) and X-ray diffraction (XRD).

---

[*] Corresponding author. Tel. +1-613 584 3311; fax: +1-613 584 1220.
E-mail address: sunders@aecl.ca (S. Sunder).

PII: S0022-3115(99)00242-1

2. Experimental

2.1. Materials

Two kinds of $(Th,U)O_2$ samples were used in this study – called here WL pellets and CRL pellets [10]. The WL pellets contained 2.4% UO_2 in ThO_2. The UO_2 used in the WL pellets was natural UO_2, i.e., 0.7% ^{235}U. The CRL pellets contained 1.5% UO_2 (93% ^{235}U) in ThO_2. The pellets were made by mixing ThO_2 and UO_2 powders, followed by cold pressing and sintering at around 1700°C. These pellets had density ~9.64 g cm^{-3}, diameter ~14.5 mm, height ~14.5 mm, average weight ~22.5 g. (Note that the theoretical density of ThO_2 and UO_2 are 9.86 and 10.96 g/cm^3, respectively [11].) UO_2 pellets used in reference experiments were standard production CANDU fuel pellets.

The electrical resistance of all the $(Th,U)O_2$ pellets obtained for this study was very high [10]. Therefore, we did not use electrochemical techniques, like those used in our studies on UO_2 corrosion, to study the corrosion of $(Th,U)O_2$. The corrosion of $(Th,U)O_2$ was investigated by studying changes in its surface chemistry and by measuring the amount of uranium dissolved during a corrosion test.

The pellets were cut with a diamond saw to obtain ~4.5 mm thick disks for the corrosion experiments. Water was used as the lubricant and coolant in the cutting process. The sample disk was mechanically polished on all sides, including the rim, using a 600-grit SiC paper to expose a fresh surface before all corrosion experiments. Polishing was carried out using water as the lubricant. The disk was washed with water and methanol to remove the loose particles and organic film that may have formed on the surface during polishing.

The water used for washing and corrosion tests was purified by passing distilled water through a Millipore milli-R06+ unit with organic and inorganic removal cartridges. The purified water had a specific resistance of 18.2 MΩ cm and a pH of ~5.5 – from CO_2 dissolved from the air. The methanol used was of analytical reagent grade purity, obtained from AnalaR, BDH. Corrosion experiments were carried out in purified water pH ~5.5, and in slightly acidic water, pH ~3. The lower pH solution was obtained by adding a small amount of nitric acid, Fisher Scientific Reagent ACS grade, to water. The pH was measured using a Fisher Accumet pH meter 25 – calibrated using buffer solutions of pH 7.0 and 4.0, obtained from Fisher.

2.2. Corrosion experiment

Room temperature, open air, corrosion tests were carried out using 50 ml-Pyrex beakers as the reaction vessels. The reaction vessel was placed in a larger beaker, partially filled with water, that was covered with a cardboard carton standing on three rubber bungs. This allowed a constant supply of fresh, clean air without causing significant loss of water from the reaction vessel by evaporation.

High temperature (~95°C) tests were carried out using wide-mouth Teflon bottles (capacity 90 ml) as the reaction vessels. Corrosion tests were started by adding 10 ml of water (or water containing nitric acid) to the reaction vessel containing a polished, washed, dried and weighed disk of $(Th,U)O_2$. The sealed bottle was placed in a heated sand bath in an oven at ~95°C [10,12]. Control tests were conducted using a UO_2 disk in place of a $(Th,U)O_2$ disk, and without any disk. All tests were carried out for a period of about six days (Table 1). After this period, the reaction vessel was removed from the oven and cooled to room temperature on the laboratory bench. The sample disk was removed from the solution, mounted on an XPS sample holder, pumped down to degas, and analyzed using XPS as described below (Section 2.3). The sample disk was weighed immediately after the XPS analysis to determine the weight change during the corrosion test. There was a very small decrease (less than a few tenths of a milligram) in the weight of the disk during the corrosion tests. The sample disk was submitted for XRD analysis (Section 2.4) after weighing.

The pH and volume of solution remaining in the reaction vessel were measured and the solution analyzed for uranium. Uranium concentration in the solution was determined by the standard addition method using FLURAN (a buffered inorganic complexing agent) and a Scintrex Fluorescence Uranium Analyzer UA-3 [13].

2.3. X-ray photoelectron spectroscopy

XPS spectra were recorded using a PHI-5300 ESCA system [14]. The sample disk was mounted on an XPS specimen holder and brought into the side-arm of the spectrometer where it was pumped for >10 min before introducing it into the spectrometer. The sample was pumped in the side arm to reduce excessive degassing from the sample in the spectrometer. The spectra were excited using Mg Kα X-rays (generated by operating the anode at 15 kV and 20 mA, i.e., at a power of 300 W) and filtered through an Al window. The binding energy scale of the spectrometer was calibrated using known energies of bands in the spectra of noble metals [12,14].

2.4. X-ray diffraction

A Rigaku Rotaflex X-ray diffractometer, equipped with a 12 kW rotating-anode Cu Kα X-ray source and a diffracted-beam graphite monochromator, was used to obtain the XRD patterns [12,14]. The sample disk was placed in a specially designed brass sample-holder to record the XRD data from its surface. XRD data were

Table 1
Summary of $(ThU)O_2$ corrosion experiments[a]

Experiment #	Sample	Conditions of experiment	V_i (ml)	V_f (ml)	pH_i	pH_f	$[U]_f$ (μg l^{-1})	Dissolution rate[a] (mg m^{-2} d^{-1})
A	WL $(Th, U)O_2$	150 h, Room temp., open air	10.0	6.7	3.04	2.87	23	0.05
B	WL $(Th,U)O_2$	148 h, Room temp., open air	10.0	6.7	3.01	2.97	31	0.07
C	WL $(Th,U)O_2$	144.5 h, 96°C, Sealed bottle	10.0	9.5	3.11	2.98	100	0.34
D	CRL $(Th,U)O_2$	144.5 h, 95°C, Sealed bottle	10.0	9.6	3.00	3.03	1300	4.4
E	CRL $(Th,U)O_2$	143 h, 95°C, Sealed bottle	10.0	9.8	5.55	4.69	260	0.9
F	UO_2, V3	140 h, 95°C, Sealed bottle	10.0	9.8	3.02	3.2	97 000	350
G	UO_2, V25	140 h, 95°C, Sealed bottle	10.0	9.8	3.02	3.15	88 000	310
H	Blank, #2	140 h, 95°C, Sealed bottle	10.0	10	3.02	3.02	1	–
I	Blank, #50	140 h, 95°C, Sealed bottle	10.0	9.8	3.02	2.98	1	–
J	UO_2, V3	141 h, Room temp., sealed bottle	10.0	10	5.75	5.78	430	1.6
K	UO_2, V25	141 h, Room temp., sealed bottle	10.0	10	5.75	5.85	410	1.5
L	Blank, #20	141 h, Room temp, sealed bottle	10.0	10	5.75	5.76	19	–
M	Blank, #10	141 h, Room temp., sealed bottle	10.0	10	5.75	5.76	10	–

[a] Dissolution rates calculated using geometric surface area, see text for the method for correcting for surface roughness. See text for explanation of the column headings.

obtained from the same surface as that used for the XPS analysis. The XRD data were obtained using a scanning rate of 1° min^{-1}.

3. Results and discussion

3.1. X-ray diffraction

Fig. 1 shows the XRD pattern of a polished disk of $(Th,U)O_2$, from a WL pellet, used in experiment A (Table 1). The bottom part of this figure compares the observed pattern of $(Th,U)O_2$ with the literature pattern of synthetic ThO_2 [15]. There is good agreement between the two patterns; nearly all of the observed peaks could be assigned to the ThO_2 pattern. Only one extremely weak feature, observed at $2\theta = 13.71$ ($d = 6.45$ Å) in the XRD pattern (Fig. 1), could not be assigned to the ThO_2 pattern. Distinct peaks for uranium oxides were not seen in the XRD pattern. The information about the oxidation state of uranium in the test specimens was obtained using XPS, as discussed below.

An analysis of all the observed diffraction peaks, with $60^\circ < 2\theta < 120^\circ$ (both $K\alpha_1$ and $K\alpha_2$) in Fig. 1, gave the value of the unit-cell parameter $a = 5.5941(3)$ Å for the WL pellet containing 2.4% UO_2 in ThO_2. The figure in parentheses is the estimated standard deviation in the last significant figure. Similar analyses were carried out on five different UO_2 specimens and gave values of the unit-cell parameter a ranging between 5.4700 and 5.4704 Å. Our experimental values of unit-cell parameter a for UO_2 are in excellent agreement with the literature value of 5.4704 ± 0.0003 Å reported by Cohen and Berman [16].

Cohen and Berman also determined values of unit-cell parameter for ThO_2, $a = 5.5975 \pm 0.0002$ Å; and for $(Th_{0.899}U_{0.101})O_{2.00}$, $a = 5.5846(3)$ Å. One obtains a value of unit cell parameter $a = 5.5944$ Å for $(Th_{0.976}U_{0.024})O_2$ by interpolating between the values of UO_2 and ThO_2, or by interpolating between the values for $(Th_{0.899}U_{0.101})O_{2.00}$ and ThO_2. This calculated value for $(Th_{0.976}U_{0.024})O_2$ is in good agreement with the experimental value obtained above. This suggests that the $(Th,U)O_2$ disk used in experiment A is a homogeneous solid solution of the stated composition.

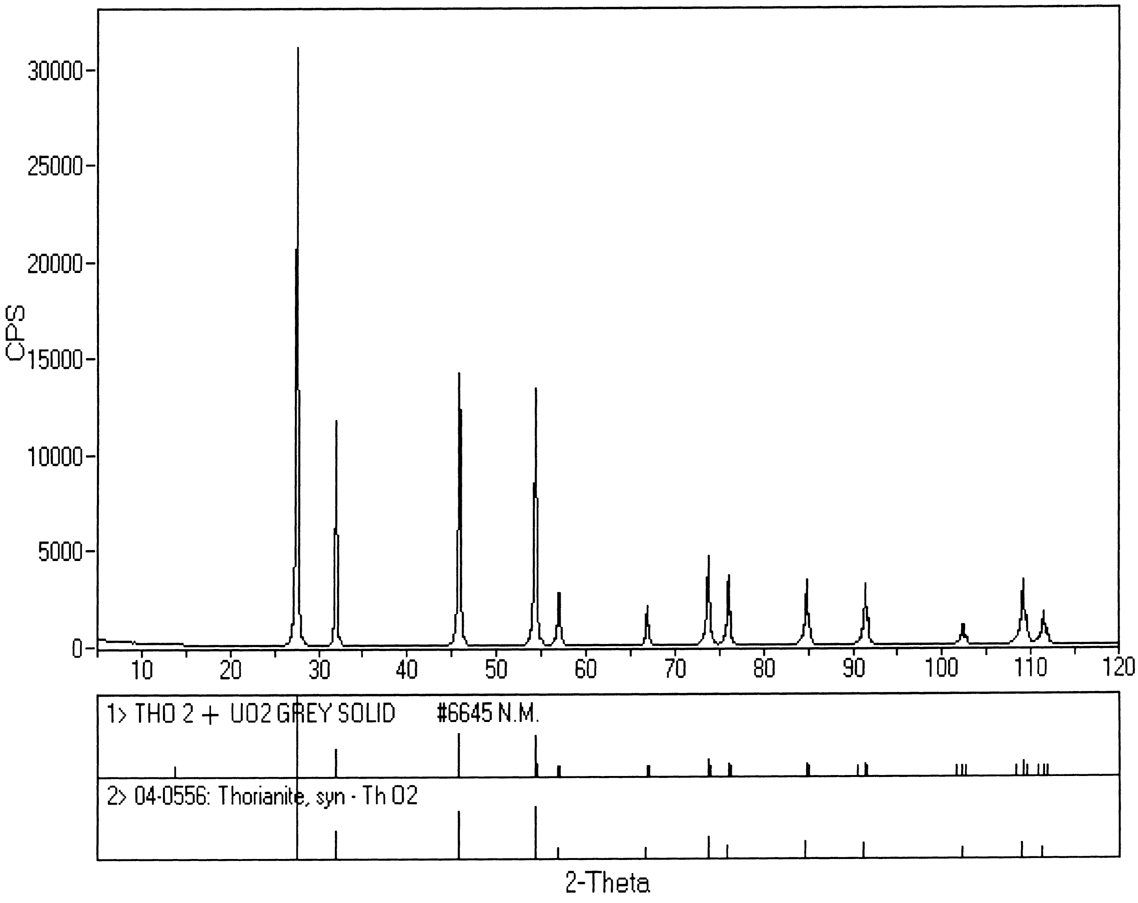

Fig. 1. XRD pattern of a freshly polished $(Th,U)O_2$ disk containing 2.4% UO_2, (sample # 6645 N.M.), top; and comparison of the observed pattern with the literature pattern for synthetic thorianite, ThO_2, bottom.

3.2. X-ray photoelectron spectroscopy

XPS spectra of the $(Th,U)O_2$ disks were recorded before and after the corrosion experiments. Low-resolution survey spectra, for the 0–1100 eV region, were recorded to determine the elements present in the pellet surface. High-resolution spectra were recorded for C 1s, O 1s, Th 4f, Th 5d, U 4f, and the valence region (0–20 eV) to determine the chemical state of these elements. (The C 1s band arises from the ubiquitous hydrocarbons present on solid surfaces.) The XPS spectra of $(Th,U)O_2$ disks showed severe charging owing to the non-conducting nature of the sample, as discussed above. The C 1s band with a binding energy value of 284.8 eV was used to correct for charging effects [14].

Fig. 2 shows a survey spectrum of a polished disk, from a WL pellet, used in experiment A (Table 1). The bands seen in this spectrum can be assigned to thorium, uranium, oxygen and carbon peaks [17,18]. Figs. 3, 4 and 5 show typical high-resolution spectra for O 1s, Th 4f, and U 4f regions, respectively, for the same disk. Note that Figs. 2–5 are plotted using a charge correction obtained from the spectrum of the C 1s band, as discussed above. The O 1s band in the spectrum of the freshly polished sample (Fig. 3) suggests that most of the intensity of this band arises from the oxide (O^{2-}) moieties, i.e., from a peak centered around 529.8 eV. The weak shoulders seen on the high binding energy side of this band most probably arise from OH^- and H_2O moieties present on the surface. Analyses of the O 1s

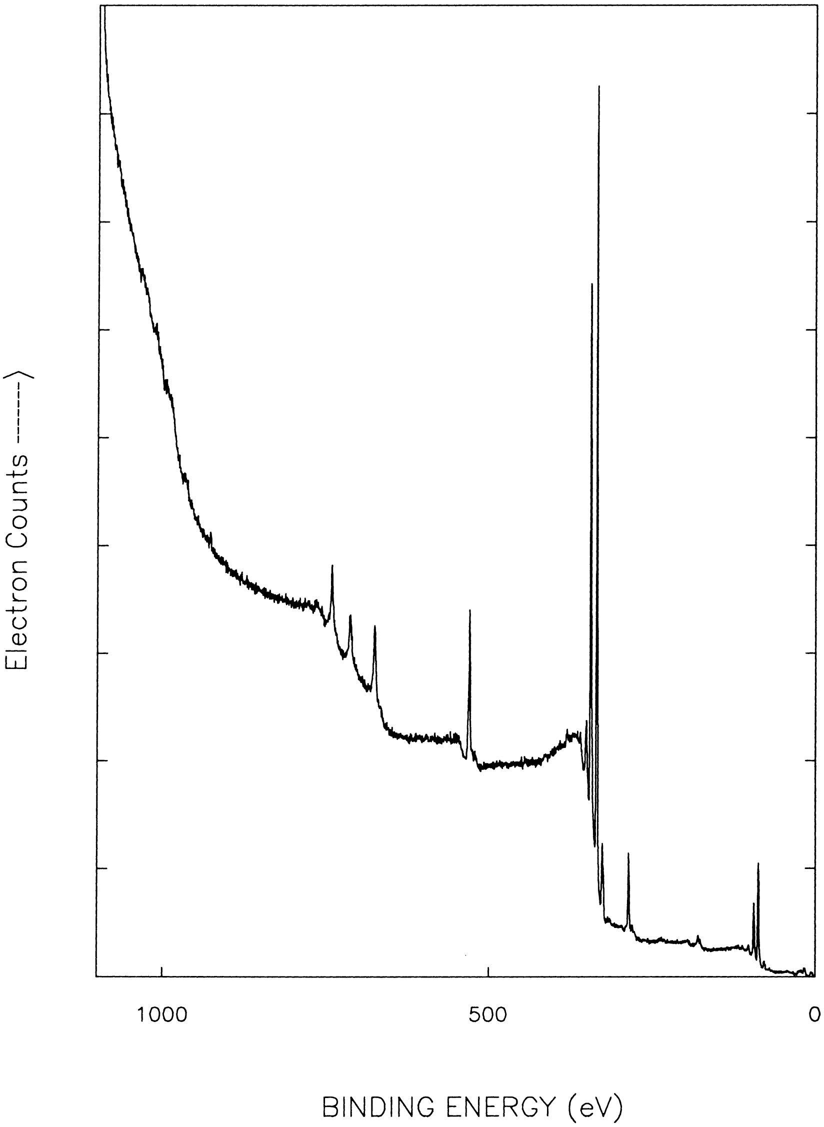

Fig. 2. Survey XPS spectrum of a freshly polished $(Th,U)O_2$ disk containing 2.4% UO_2.

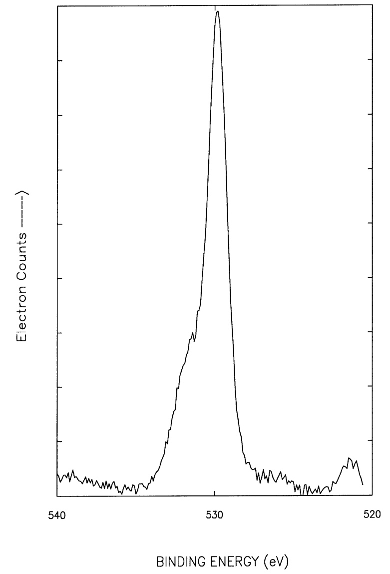

Fig. 3. High-resolution XPS spectrum for the O 1s region of a freshly polished (Th,U)O_2 disk containing 2.4% UO_2.

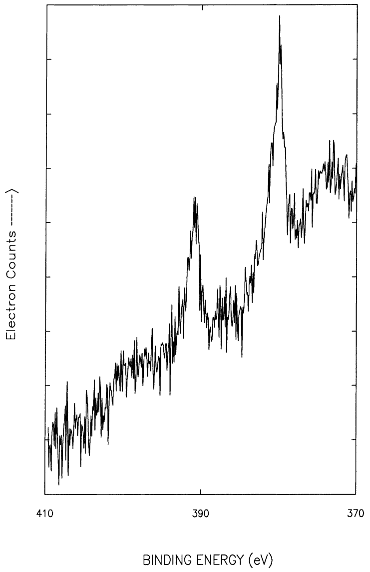

Fig. 5. High-resolution XPS spectrum for the U 4f region of a freshly polished (Th,U)O_2 disk containing 2.4% UO_2.

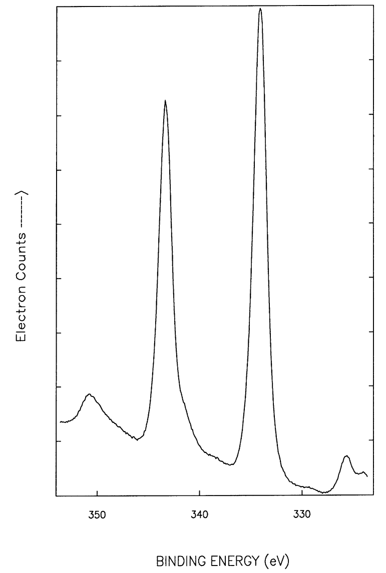

Fig. 4. High-resolution XPS spectrum for the Th 4f region of a freshly polished (Th,U)O_2 disk containing 2.4% UO_2.

bands into O^{2-}, OH^- and H_2O components, according to the procedure described elsewhere [14], showed that the fraction of the OH^- and H_2O species was much higher in the spectrum of a corroded sample than in the spectrum of the freshly polished sample.

The binding energies of the Th 4f bands (Fig. 4) and Th 5d bands in the freshly polished or corroded (Th,U)O_2 samples were equal to those expected for ThO_2 [17,18]. However, the binding energies of the U 4f bands were slightly higher in the spectra of the corroded samples than those in the spectrum of a freshly polished sample. The binding energies of the U 4f bands are very sensitive to the chemical state of the uranium atom and increase with an increase in its oxidation state. (Fig. 5 shows the spectrum for the U 4f bands for a freshly polished (Th,U)O_2 sample.) For example, the U $4f_{7/2}$ band occurs at ~379.9 eV in UO_2 and at ~381.2 eV in UO_3 ([14] and references therein). Therefore, the increase observed in the binding energies of the U 4f bands of the samples, after the corrosion tests, indicates that the uranium present in the surface of these samples underwent some oxidation during the tests.

We have developed a procedure to obtain the relative amounts of U^{6+} and U^{4+} in the surface of a sample containing uranium oxides from an analysis of its U $4f_{7/2}$ band [19,20]. This procedure was used to determine the relative amounts of U^{6+} and U^{4+} in the samples used in the tests, Table 2. This table also contains U^{6+}/U^{4+} ratios for freshly polished (Th,U)O_2 and UO_2 disks for comparison purposes. In general, there was an increase in the U^{6+}/U^{4+} ratio during corrosion of (Th,U)O_2 disks in aerated solutions. The average value of the U^{6+}/U^{4+} ratio is ~0.3 in acidic solutions (pH ~3) and ~0.6 in near neutral (pH ~5.5) solutions. We believe that the lower values of the U^{6+}/U^{4+} ratio, for the samples corroded in acidic water, is due to the increased dissolution of U^{6+} species in acidic solutions [8]. This conclusion is consistent with corrosion rate results discussed below.

Table 2
$(Th,U)O_2$ corrosion experiments: XPS results

Experiment #	Sample disk	Conditions of experiment	pH_i	pH_f	U^{6+}/U^{4+} ratio from XPS[a]
	UO_2, V25	Freshly polished			0.07
	CRL $(Th,U)O_2$	Freshly polished			0.09
A	WL $(Th,U)O_2$	150 h, room temp., open air	3.04	2.87	0.21
B	WL $(Th,U)O_2$	148 h, room temp., open air	3.01	2.97	0.14
C	WL $(Th,U)O_2$	144.5 h, 96°C, sealed bottle	3.11	2.98	0.35
D	CRL $(Th,U)O_2$	144.5 h, 95°C, sealed bottle	3.00	3.03	0.51
E	CRL $(Th,U)O_2$	143 h, 95°C, sealed bottle	5.55	4.69	0.33
F	UO_2, V3	140 h, 95°C, sealed bottle	3.02	3.2	0.59
G	UO_2, V25	140 h, 95°C, sealed bottle	3.02	3.15	0.57
J	UO_2, V3	141 h, room temp., sealed bottle	5.75	5.78	0.77
K	UO_2, V25	141 h, room temp., sealed bottle	5.75	5.85	0.57

[a] The uncertainty in the U^{6+}/U^{4+} ratio values is estimated to be ±10% for UO_2 samples and ±20% for $(Th,U)O_2$ samples. The higher uncertainty for the $(Th,U)O_2$ samples is because of the lower signal-to-noise ratio of uranium bands (resulting from low concentration of uranium atoms) in these samples.

3.3. Corrosion rates

Corrosion rates of $(Th,U)O_2$ and UO_2 disks in different tests were calculated from the final concentration of uranium in the solution at the end of the corrosion tests, Table 1. These rates were calculated using equation

$$\mathrm{DR} = (U_f V_f k\ 24)/(tA\ 100), \tag{1}$$

where DR is the dissolution rate (mg m^{-2} d^{-1}), U_f the uranium concentration (µg l^{-1}), V_f the final volume (ml), t the time of corrosion test (h), A the area of the disk (cm^2), and k is the conversion factor to calculate dissolved UO_2 from measured amount of uranium, i.e., = (270/238) = 1.1344.

The dissolution rates are calculated in units of mg m^{-2} d^{-1} to facilitate a comparison of uranium dissolution rates obtained in this work with the recent studies on UO_2 fuel dissolution carried out for the nuclear fuel waste management programs (see Fig. 6). The relative precision (2s) of the uranium concentrations shown in Table 1 is ±20%.

The dissolution rates given in Table 1 were calculated using the geometric area of the sample disk, i.e., 5.35 cm^2. To obtain the *actual* area of a solid the geometric area is multiplied by the roughness factor. The roughness factor for UO_2 disks is believed to be ~3 [21–23]. If one were to use the same roughness factor for $(Th,U)O_2$ as that for UO_2, the dissolution rates shown in Table 1 will be reduced by a factor of three.

The use of Eq. (1) to calculate the UO_2 dissolution rate implies that the final uranium concentration in the aqueous phase is still unsaturated with respect to solid U-containing phases, i.e., there is no significant re-precipitation of dissolved uranium [24]. This is a reasonable assumption for tests with the $(Th,U)O_2$ samples because of the low uranium concentrations seen in these tests (Table 1). Fig. 6 compares the dissolution rates for UO_2 in aerated, near neutral pH, water at room temperature obtained in this work (experiments J and K) with the results reported in literature [22,24–28]. The dissolution rates shown are for the actual surface area of the fuel (see above). The dissolution rate reported by Shoesmith and Sunder [25] was obtained using electrochemical techniques – all others were obtained by chemical analysis of the solution phase. The dissolution rates were obtained by different workers using different type of fuel samples, i.e., unirradiated CANDU fuel (UO_2) pellets were used by Thomas and Till [24] and by Shoesmith and Sunder [25], unirradiated SIMFUEL (SIMulated

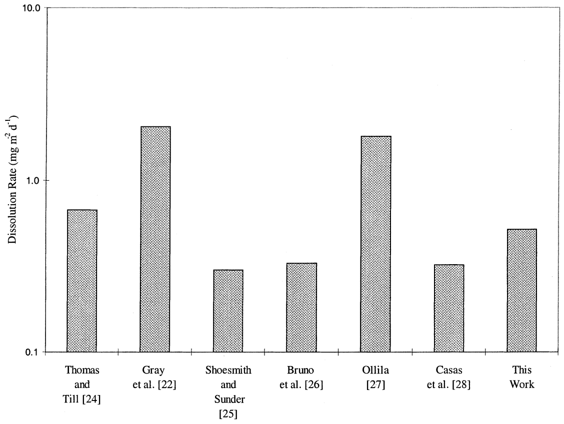

Fig. 6. Comparison of dissolution rates of UO_2 fuel obtained by different workers in aerated, non-complexing, near neutral aqueous solutions at room temperature (see text for the nature of the fuel samples used in different studies).

used FUEL) pellets were used by Bruno et al. [26] and by Ollila [27], unirradiated UO_2 particles were used by Casas et al. [28], and used LWR fuel particles were used by Gray et al. [22]. Also, the solutions used in these studies were of slightly different compositions although all of them had pH values close to neutral and did not contain high concentrations of strongly complex anions, such as CO_3^{2-}. There are several reports which discuss the factors which affect the dissolution rates of UO_2 in water (e.g., see Refs. [7,23,29]). It is sufficient to note here that there is a good agreement between the results obtained in this work (for UO_2 dissolution in aerated solutions) and those reported in the literature. This gives confidence in the method used in this work to obtain the dissolution rates of $(Th,U)O_2$.

A comparison of the dissolution rates for $(Th,U)O_2$ and UO_2 samples in pH ~3 solution at ~95°C (Table 1) shows that the rate of uranium dissolution from $(Th,U)O_2$ is much lower than that from UO_2. In particular, the dissolution rate of uranium from WL $(Th,U)O_2$ is lower by a factor of ~970 than that from UO_2 under these conditions, experiment C compared to experiments F and G. As the UO_2 concentration in the solid sample used in experiment C is 2.4%, the reduction in the uranium dissolution rate is more than 20 times greater than that expected solely from a decrease in the uranium concentration in the solid phase. We have not attempted a similar quantitative comparison of uranium dissolution rates from $(Th,U)O_2$ and UO_2 at room temperature because of the exceedingly low uranium dissolution rates from $(Th,U)O_2$ at pH ~3, Experiments A and B in Table 1. UO_2 solubility is lower at pH 5.5 than that at pH 3 [8]. It is clear from the data shown in Table 1 that the uranium dissolution rates in water are much lower from $(Th,U)O_2$ than those from UO_2. These results are in agreement with the results of Grandstaff [30] who carried out an extensive study on the dissolution of uraninite minerals in water. Grandstaff also observed much lower (about 2–3 orders of magnitude) uranium dissolution rates in aerated water for uraninite minerals containing ThO_2 than those for uraninite minerals with little ThO_2. It may be noted here that the $(Th,U)O_2$ samples used in this work were mostly ThO_2 (>97% ThO_2), with small amounts of UO_2, while those used by Grandstaff [30] were mainly UO_2 (>70%). (The maximum ThO_2 in the samples investigated by Grandstaff was less than 20%.)

There are several factors in addition to the lower concentration of UO_2 in the solid samples which may be contributing to the decrease observed in the UO_2 dissolution rate for a $(Th,U)O_2$ sample. Both ThO_2 and UO_2 solids have fluorite structure [6] and thorium and uranium ions can easily replace each other in the fluorite lattice. However, replacement of a uranium ion by a thorium ion in the solid matrix will change its semiconductor properties [30]. Changes in the semiconductor properties of a metal oxide affect its solubility and dissolution rate. It has been suggested that the major difference between slow- and fast-dissolving oxides appears to be the intrinsic conductivity of the solid, which makes solid-state charge transfer rate-limiting for slowly dissolving oxides. (Appendix A in Ref. [25] gives a concise review of relationships between dissolution rates and solid-state properties of metal oxides.) Also, it has been shown that the dissolution of UO_2 in aerated solutions is an electrochemical process [20,25,29]. Therefore, we believe that the lower dissolution rates observed for $(Th,U)O_2$ fuel and thoria containing are probably related to the lower electrical conductance observed for these solids (Section 2). Clearly, more work is required if one has to gain a quantitative insight into the relationship between the dissolution rate and composition of $(Th,U)O_2$.

The results obtained in this work show that the uranium dissolution rate from $(Th,U)O_2$ fuel, with UO_2 present as a solid solution in ThO_2, will be much lower than that from UO_2 fuel. The release rate of fission products (FPs) from used fuel into liquid water is governed by the dissolution rate of the fuel as >90% of the FPs are present within the fuel grains [29]. Therefore, the release of most of the radioactive FPs would be much lower from used $(Th,U)O_2$ fuel than that from used UO_2 fuel. Hence, the used $(Th,U)O_2$ fuel should be a suitable waste form for direct geological disposal. It should be noted, however, that the results obtained in this study and those reported by Grandstaff [30] were obtained from experiments carried out in solutions containing dissolved oxygen as the oxidant and do not take into account the effects of water radiolysis on UO_2 dissolution from $(Th,U)O_2$ fuel. It has been shown by several authors that the radical oxidants formed during water radiolysis are much more effective in increasing the oxidation and dissolution rates of UO_2 fuel than the dissolved oxygen [7,23,25,31–33]. Gromov [31] has shown that the water radiolysis products increase the dissolution rate of not only UO_2 but also of U_3O_8. Sunder et al. [32] and Christensen et al. [33] have shown that a significant increase in the dissolution rate of UO_2, in an aerated solution occurs when the solution is exposed to gamma radiation. [1] Therefore, it would be prudent to carry out selected experiments on the effects of water radiolysis on uranium dissolution from $(Th,U)O_2$ fuel.

---

[1] Fig. 2 in Ref. [32] gives a good illustration of the increase in the dissolution rate of UO_2 caused by water radiolyis products. The figure shows the corrosion potential of a UO_2 electrode in aerated and argon-purged solutions. (Corrosion potential is a measure of the dissolution rate of UO_2 [25].) The corrosion potential of the UO_2 electrode showed a sharp increase, due to the increased corrosion/dissolution caused by the water radiolysis products, when the solution was exposed to gamma radiation.

4. Summary and conclusion

It is possible to prepare $(Th,U)O_2$ pellets that behave like *solid solutions* by mixing ThO_2 and UO_2 powders, followed by cold pressing and sintering at 1700°C.

The uranium in the surface of $(Th,U)O_2$ specimens undergoes oxidation as if it was present in *pure* UO_2. However, the leach rate of uranium from a properly prepared $(Th,U)O_2$, i.e., with UO_2 present as a solid solution in ThO_2 matrix, is reduced by a factor greater than that expected solely from the decrease in the uranium concentration in the solid phase.

A properly prepared $(Th,U)O_2$ fuel can be an acceptable waste-form for permanent geological disposal. Studies on the effects of water radiolysis on the uranium dissolution rates from $(Th,U)O_2$ are recommended to confirm the above conclusions.

Acknowledgements

We are grateful to P. Taylor for help in the analysis of XRD data, and thank R.J. Lemire and J. Sullivan for comments on a draft of the manuscript. Technical assistance of D. Doern in recording XRD data is acknowledged. AECL # 12057.

References

[1] P.G. Boczar, G.R. Dyck, J.D. Sullivan, R.J. Ellis, R.T. Jones, P. Taylor, A fresh look at thorium fuel cycles in CANDU reactors, Presented at IAEA Advisory Group Meeting on Thorium Fuel Cycle Perspectives, 1997.

[2] A.R. Dastur, A.S. Gray, N. Gagnon, D.B. Buss, R.A. Verrall, P.G. Lucuta, H.R. Andrews, Annihilation of Plutonium in CANDU Reactors, Presented at the IAEA Technical Committee Meeting on Unconventional Options for Pu Disposition, held at Obninsk, Russia, November 1994.

[3] H.T. Akie, T. Muromura, H. Takano, S. Matsuura, Nucl. Technol. 107 (1994) 182.

[4] D. Langmuir, J.S. Herman, Geochim. Cosmochim. Acta 44 (1980) 1753.

[5] R.J. Lemire, F. Garisto, The solubility of U, Np, Pu, Th and Tc in a geological disposal vault for used nuclear fuel, Atomic Energy of Canada Limited Report, AECL-10009 (1989).

[6] P. Taylor, W.H. Hocking, L.H. Johnson, R.J. McEachern, S. Sunder, Nucl. Technol. 116 (1996) 222.

[7] S. Sunder, D.W. Shoesmith, Chemistry of UO_2 fuel dissolution in relation to the disposal of used nuclear fuel, Atomic Energy of Canada Limited Report, AECL-10395 (1991).

[8] I. Grenthe, J. Fuger, R.J.M. Konings, R.J. Lemire, A.B. Muller, C. Nguyen-Trung, H. Wanner, in: H. Wanner, I. Forest (Eds.), Chemical Thermodynamics of Uranium, vol. 1: Chemical Thermodynamics, North-Holland, Amsterdam, 1992.

[9] R.W. Dyck, R. Taylor, D.G. Boase, Dissolution of $(Th,U)O_2$ in nitric acid hydrofluoric acid solutions, Atomic Energy of Canada Limited Report, AECL-5957 (1977).

[10] S. Sunder, N.H. Miller, Corrosion of $(Th,U)O_2$ fuel at room temperature and near 100°C in near neutral and acidic water (pH 3), Atomic Energy of Canada Limited Report, AECL-11967 (1999).

[11] D.R. Lide (Ed.), CRC Handbook of Chemistry and Physics, 71st Ed., 1990.

[12] S. Sunder, N.H. Miller, Corrosion of UN in water, Atomic Energy of Canada Limited Report, AECL-11656 (1996).

[13] Scintrex, Analytical measurements and instruments, analytical procedure for UA-3 uranium analysis, Application Brief 79-2. Concord, Ontario, Canada, 1985.

[14] S. Sunder, N.H. Miller, XPS, XRD and SEM study of oxidation of UO_2 by air in gamma radiation at 150°C, Atomic Energy of Canada Limited Report, AECL-11351, COG-95-296 (1995).

[15] ICDD, Powder diffraction files, International Center for Diffraction Data, Newton Square, PA, USA, 1994.

[16] I. Cohen, R.H. Berman, J. Nucl. Mater. 18 (1966) 77.

[17] C.D. Wagner, W.M. Riggs, L.E. Davis, J.F. Moulder, G.E. Muilenberg, Handbook of X-ray Photoelectron Spectroscopy, Perkin–Elmer, Eden Prairie, MN, 1979.

[18] J.F. Moulder, W.F. Stickle, P.E. Sobol, K.D. Bomben, in: J. Chastain (Ed.), Handbook of X-ray Photoelectron Spectroscopy, Perkin–Elmer Corp., Physical Electronics Division, Eden Prairie, MN, USA, 1992.

[19] S. Sunder, G.D. Boyer, N.H. Miller, J. Nucl. Mater. 175 (1990) 163.

[20] S. Sunder, D.W. Shoesmith, M.G. Bailey, F.W. Stanchell, N.S. McIntyre, J. Electroanal. Chem. 130 (1981) 163.

[21] D.W. Shoesmith, S. Sunder, M.G. Bailey, G.J. Wallace, Corros. Sci. 29 (1989) 1115.

[22] W.J. Gray, H.R. Leider, S.A. Steward, J. Nucl. Mater. 190 (1992) 46.

[23] D.W. Shoesmith, J.C. Tait, S. Sunder, W.J. Gray, S.A. Steward, R.E. Russo, J.D. Rudnicki, Factors affecting the differences in reactivity and dissolution rates between UO_2 and spent nuclear fuel, Atomic Energy of Canada Limited Report, AECL-11515, COG-95-581 (1996).

[24] G.F. Thomas, G. Till, Nucl. Chem. Waste Manag. 5 (1984) 141.

[25] D.W. Shoesmith, S. Sunder, J. Nucl. Mater. 190 (1992) 20.

[26] J. Bruno, I. Casas, A. Sandino, J. Nucl. Mater. 190 (1992) 61.

[27] K. Ollila, J. Nucl. Mater. 190 (1992) 70.

[28] I. Casas, J. Gimenez, J. De Pablo, M.E. Torrero, Mater. Res. Soc. Symp. Proc. 294 (1993) 67.

[29] L.H. Johnson, D.M. Leneveu, F. King, D.W. Shoesmith, M. Kolar, D.W. Oscarson, S. Sunder, C. Onofrei, J.L. Crosthwaite, The disposal of Canada's nuclear fuel waste: a study of post-closure safety of in-room emplacement of used CANDU fuel in copper containers in permeable plutonic rock, vol. 2, Atomic Energy of Canada Limited Report, AECL-111494-2, COG-95-552-2 (1996).

[30] D.E. Grandstaff, Econom. Geol. 71 (1976) 1493.

[31] V. Gromov, Rad. Phys. Chem. 18 (1981) 135.

[32] S. Sunder, D.W. Shoesmith, H. Christensen, M.G. Bailey, N.H. Miller, Mater. Res. Soc. Symp. Proc. 127 (1989) 317.

[33] H. Christensen, R. Forsyth, R. Lundqwist, L. Werme, Radiation induced dissolution of UO_2, Studsvik Report NS-90/85, Studsvik Nuclear, Nykoping, Sweden, 1990.